Serdica Journal of Computing 19(1), 2025, pp. 17-35, 10.55630/sjc.2025.19.17-35
Published by Institute of Mathematics and Informatics, Bulgarian Academy of Sciences

Rademacher-Based Pixel and Color-Channel Selection for Robust Image Steganography

Spartak Sirakanyan[1], Sergo Episkoposyan[2]

[1]Institute for Informatics and Automation Problems,
National Academy of Sciences of the Republic of Armenia, Armenia
spartak.sirakanyan@iiap.sci.am

[2]National Polytechnic University of Armenia, Armenia
sergo.episkoposyan@polytechnic.am

Abstract

This paper proposes a novel image steganographic method based on discrete Rademacher functions combined with Least Significant Bit (LSB) embedding. Unlike conventional sequential LSB techniques, which modify pixel values in a deterministic scan order, the proposed approach introduces a mathematically structured selection mechanism that governs both spatial embedding locations and, in the case of color images, channel selection. The performance of the proposed method is evaluated using standard benchmark images, including grayscale and color versions of the Lena, Tank, and Pepper datasets at a resolution of 512 × 512 pixels. The quality of stego-images is measured using Peak Signal-to-Noise Ratio (PSNR) and Structural Similarity Index (SSIM), ensuring both pixel-level accuracy and perceptual similarity assessment. Experimental results demonstrate that the proposed method maintains PSNR values above conventional acceptability thresholds and SSIM values close to unity across various embedding rates. Comparative analysis with classical sequential LSB embedding confirms that the proposed approach achieves comparable or improved imperceptibility, particularly in color images due to distributed channel embedding. The results indicate that Rademacher-based LSB steganography offers a favorable trade-off between embedding capacity, visual quality, and security.

Keywords: steganography, Rademacher-based embedding, LSB, color channels, pixel selection, steganalysis, orthogonal methods

ACM Computing Classification System 2012: Mathematics of computing → Information theory → Coding theory, Information systems → Information storage systems

Mathematics Subject Classification 2020: 68U10, 94A08, 42C10

Received: May 4, 2026, *Accepted:* June 7, 2026, *Published:* June 10, 2026
Citation: Spartak Sirakanyan, Sergo Episkoposyan, Rademacher-Based Pixel and Color-Channel Selection for Robust Image Steganography, Serdica Journal of Computing 19(1), 2025, pp. 17-35, https://doi.org/10.55630/sjc.2025.19.17-35

1 Introduction

Information security has always been a critical concern for humans. Long before the advent of computers and digital communication, people sought ways to hide messages from unauthorized access. The practice of concealing information, known today as steganography [1, 2], has a rich historical background.

Historically, steganography was applied using a variety of creative methods. One of the earliest known examples is the use of invisible inks and secret writing in manuscripts. Another classical method involved hiding messages in books, often referred to as book ciphers. In this approach, a pre-agreed book is used as a key, and the secret message is encoded by specifying the page number, line number, word number, and even letter position within a word. Only someone who possesses the correct book can decode the hidden message.

Such techniques were widely used in diplomacy, espionage, and wartime communication. Although analog in nature, these methods laid the foundation for modern digital steganography. The main goal of steganography is to hide the very existence of a message, as opposed to cryptography, which only makes the content unreadable. In modern times, digital steganography allows embedding information within images, audio, video, or text files in ways that are imperceptible to human observers.

This paper focuses on image steganography and introduces a robust approach using Rademacher functions to select pixel positions for hiding information. Unlike classical Least Significant Bit (LSB) methods, the proposed approach distributes the hidden data in a mathematically guided, non-obvious pattern, increasing resistance against detection and analysis.

2 LSB steganography

The Least Significant Bit (LSB) steganography is one of the simplest and most widely used methods for hiding information within images.

Let the cover image have pixel intensities:

$$I = [I_1, I_2, \ldots, I_N], \quad I_k \in \{0, 1, \ldots, 255\},$$

and let the secret message be a binary sequence:

$$M = [m_1, m_2, \ldots, m_L], \quad m_k \in \{0, 1\}.$$

In LSB Figure 1 steganography, the least significant bit of each pixel is replaced with the message bit:

$$I'_k = (I_k \& 254) | m_k,$$

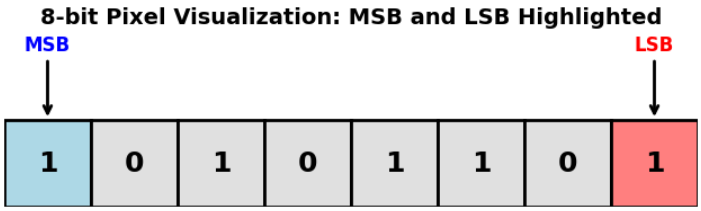

Figure 1: Visualization of an 8-bit pixel: MSB (b1, blue) and LSB (b8, red) are highlighted.

where $I_k \& 254$ clears the least significant bit of the pixel, and $|m_k$ sets the LSB to the message bit.

The Most Significant Bit (MSB) represents the highest weight in the pixel's binary representation and changing it produces a noticeable alteration in the pixel intensity. In contrast, the Least Significant Bit (LSB) has the lowest weight; modifying it results in minimal change, imperceptible to the human eye. Thus, LSB is generally preferred for hiding secret information in images, providing high capacity and imperceptibility, which makes it an effective method for image steganography.

2.1 Limitations of LSB and motivation for Rademacher-based pixel selection

Although the LSB method is simple and effective for hiding information in images, it has several limitations[3, 4]. The primary drawback is its vulnerability to statistical attacks and image processing operations. Since LSB modifies the least significant bits in a predictable order (typically sequentially across pixels), an attacker can analyze the bit patterns and potentially extract the hidden message. Furthermore, common image transformations such as compression, filtering, or cropping may destroy the hidden information.

To overcome these weaknesses, we propose using Rademacher functions to select pixel positions for embedding. The random-like properties of Rademacher functions allow for non-sequential, pseudo-random pixel selection, increasing the security and robustness of the steganographic method. By embedding information only in pixels corresponding to Rademacher function outputs (e.g., -1 positions), the hidden data becomes significantly harder to detect or manipulate, while still maintaining imperceptibility in the image.

3 Rademacher functions and their matrix representation

Rademacher functions are a family of orthogonal piecewise-constant functions defined on the interval $[0, 1)$, taking values in $\{-1, 1\}$. They are widely used in digital signal processing, steganography, and orthogonal transforms due to their simple binary structure and orthogonality.

The functions can be defined using interval partitioning as follows:

$$R_0(x) = \begin{cases} +1, & x \in [0, 1/2), \\ -1, & x \in [1/2, 1), \end{cases}$$

$$R_1(x) = \begin{cases} +1, & x \in [0, 1/4) \cup [1/2, 3/4), \\ -1, & x \in [1/4, 1/2) \cup [3/4, 1), \end{cases}$$

$$R_2(x) = \begin{cases} +1, & x \in [0, 1/8) \cup [1/4, 3/8) \cup [1/2, 5/8) \cup [3/4, 7/8), \\ -1, & x \in [1/8, 1/4) \cup [3/8, 1/2) \cup [5/8, 3/4) \cup [7/8, 1). \end{cases}$$

In general, the n-th Rademacher function $R_n(x)$ divides the interval $[0, 1)$ into 2^{n+1} equal subintervals, alternating between $+1$ and -1:

$$R_n(x) = \begin{cases} +1, & x \in \text{even-numbered subintervals}, \\ -1, & x \in \text{odd-numbered subintervals}, \end{cases} \qquad n = 0, 1, 2, \ldots$$

Properties: Each function is piecewise constant and asymmetric with respect to $x = 1/2$. Rademacher functions form a complete orthogonal basis in $L^2([0, 1])$ for step functions, but they are not complete for all continuous functions. Each $R_n(x)$ oscillates faster as n increases.

3.1 Relationship between Rademacher, Walsh, and Hadamard matrices

Rademacher functions are the building blocks for Walsh functions and Walsh–Hadamard (WH) matrices. The relationship can be demonstrated as follows:

- Each row of a Walsh–Hadamard matrix can be constructed as a product of discrete Rademacher vectors.
- Let R_n denote the n-th discrete Rademacher vector. Then the k-th row of a Walsh–Hadamard matrix [5] of size $2^n \times 2^n$ can be written as

$$WH_n[k, :] = \prod_{j=0}^{n-1} R_j^{b_j(k)}, \quad k = 0, 1, \ldots, 2^n - 1,$$

where $b_j(k)$ is the j-th bit in the binary representation of k. In other words, each WH row is a Kronecker product of selected Rademacher vectors.

- Hadamard matrices are a specific orthogonal matrix class with elements ± 1, often defined recursively by

$$H_1 = [1], \quad H_{2n} = \begin{bmatrix} H_n & H_n \\ H_n & -H_n \end{bmatrix}.$$

- Walsh–Hadamard matrices are Hadamard matrices whose rows are permuted according to the sequency ordering derived from Rademacher functions.
- Rademacher functions provide the binary, oscillatory patterns.
- Walsh functions (rows) are products of Rademacher vectors, forming an orthogonal basis.
- Hadamard matrices are the structured orthogonal matrices that Walsh functions populate; they allow forward and inverse transformations for signal processing [6] and steganography.

4 Embedding a 12-bit message in a grayscale image using Rademacher functions

In this example, we demonstrate the embedding of a 12-bit secret message into a small 8×8 grayscale image using discrete Rademacher vectors to select embedding locations. This approach ensures pseudo-random, orthogonal, and less detectable placement of the message bits, compared to naive sequential LSB embedding.

4.1 Grayscale cover image

Consider an 8×8 grayscale image I where each pixel value $I_{i,j} \in [0, 255]$:

$$I = \begin{bmatrix} 34 & 120 & 45 & 200 & 90 & 180 & 60 & 240 \\ 50 & 100 & 150 & 200 & 30 & 60 & 90 & 120 \\ 80 & 160 & 40 & 220 & 110 & 70 & 180 & 240 \\ 25 & 75 & 125 & 175 & 225 & 50 & 100 & 150 \\ 60 & 120 & 180 & 240 & 30 & 90 & 150 & 210 \\ 15 & 45 & 75 & 105 & 135 & 165 & 195 & 225 \\ 10 & 50 & 90 & 130 & 170 & 210 & 250 & 30 \\ 5 & 25 & 45 & 65 & 85 & 105 & 125 & 145 \end{bmatrix}$$

This matrix serves as the cover image, in which we intend to hide the secret message. Each pixel is represented with 8 bits, allowing LSB embedding.

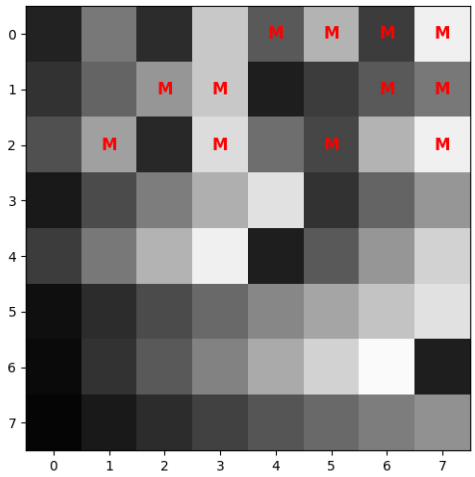

Figure 2: Rademacher-selected pixel positions for embedding a 12-bit message. Red marks indicate pixels corresponding to -1 entries in Rademacher vectors.

4.2 Secret message conversion

The secret message to embed is a 12-bit binary sequence. For example:

$$M = 101100110010.$$

This sequence is already in binary form and can be directly embedded into the selected pixels.

4.3 Discrete Rademacher vectors for pixel selection

To determine which pixels to modify, we utilize the first three discrete Rademacher vectors for $N = 8$ samples:

$$R_0 = [+1, +1, +1, +1, -1, -1, -1, -1]$$
$$R_1 = [+1, +1, -1, -1, +1, +1, -1, -1]$$
$$R_2 = [+1, -1, +1, -1, +1, -1, +1, -1]$$

The rule for embedding is as follows: pixels corresponding to -1 entries in Rademacher vectors are chosen for embedding message bits. This ensures that the embedding locations are pseudo-random, orthogonal, and evenly distributed.

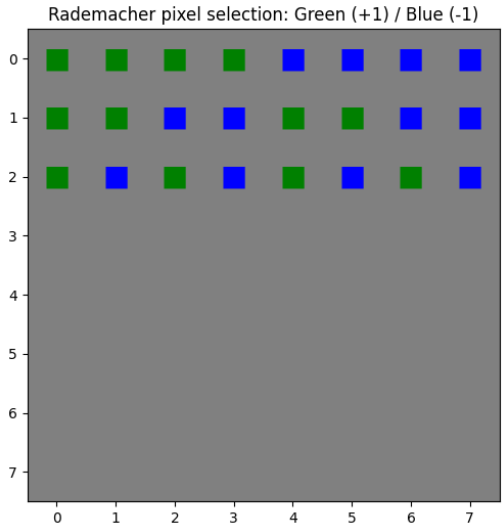

Figure 3: Rademacher-selected pixels in a color image.

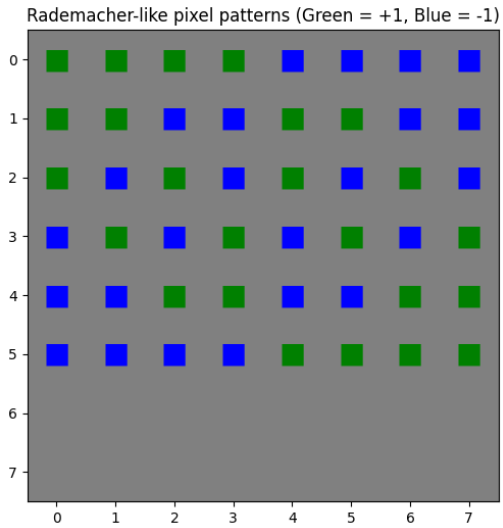

Figure 4: Alternative visualization of Rademacher-based pixel selection in a color image.

4.4 Mapping message bits to pixels

We map the message bits to the selected pixel locations in a sequential manner. For example, R_0 identifies columns $4, 5, 6, 7$ in each row, embedding the first bits of the message. R_1 identifies columns $2, 3, 6, 7$, embedding the next bits. Similarly, R_2 identifies columns $1, 3, 5, 7$, embedding the remaining bits.

The LSB of each selected pixel is modified to match the corresponding message bit. For instance, if a pixel value is 150 ('10010110' in binary) and the message bit is 1, we update it to 151 ('10010111'). The image shown in Figure 2 illustrates the Rademacher-selected pixels in the grayscale image.

4.5 Advantages of using Rademacher vectors

The use of Rademacher vectors offers several advantages over traditional LSB embedding. First, it provides a pseudo-random distribution of embedding locations, ensuring that the message bits are spread across the image in a manner that reduces detectability. Second, the orthogonal structure of Rademacher vectors minimizes correlation between message bits and the image's natural patterns, increasing the security of the hidden message. Finally, it is scalable, as it can be extended to larger images and longer messages by utilizing additional Rademacher vectors.

4.6 Message extraction

Once the message is embedded in the LSBs of the selected pixels, retrieval is performed by following the same Rademacher-based pixel selection order. First, the same discrete Rademacher vectors (R_0, R_1, R_2) are used to determine the pixel positions that were used for embedding (entries with -1). Then, for each selected pixel, its least significant bit (LSB) is extracted:

$$b = I'_{i,j} \ \& \ 1$$

where $I'_{i,j}$ is the stego-image pixel value and & denotes bitwise AND. The extracted bits are concatenated in the embedding order to reconstruct the full bitstream.

Example: If a 12-bit message was embedded, for example $M = 101100110010$ then the extracted bitstream is 101100110010. This bitstream directly represents the hidden message.

This method guarantees lossless extraction, provided that the stego-image remains unaltered. The orthogonal distribution of Rademacher-selected pixels

ensures that message bits are spread across the image, making the extraction process deterministic and the embedding less detectable.

5 Rademacher-controlled channel selection for color image steganography

In color image steganography, each pixel is represented by multiple spectral components rather than a single intensity value. In the widely used RGB color model, a pixel consists of three 8-bit channels: Red (R), Green (G), and Blue (B), each taking integer values in the range $[0, 255]$. This multi-channel structure provides additional degrees of freedom for data embedding, which can be exploited to improve both imperceptibility and security.

In this work, the Rademacher functions are employed not only to determine the spatial positions of embedding but also to control the selection of the color channel in a deterministic manner. Let $R_k(n) \in \{-1, +1\}$ denote the k-th Rademacher function evaluated at index n, where n corresponds to a linearized pixel index. The sign of the Rademacher function is used to select the color channel according to the following rule:

$$\begin{aligned} R_k(n) = -1 &\Rightarrow \text{ embedding in the Blue channel,} \\ R_k(n) = +1 &\Rightarrow \text{ embedding in the Green channel.} \end{aligned}$$

At the selected pixel position, only the least significant bit (LSB) of the corresponding color component is modified in order to embed one bit of the secret message. The red channel is intentionally excluded from the embedding process to minimize perceptual distortion, as the human visual system exhibits higher sensitivity to variations in red intensity.

This channel-selection mechanism introduces an additional layer of security, since an unauthorized observer cannot determine whether the embedded information resides in the blue or green channel without knowledge of the underlying Rademacher function. Consequently, the Rademacher index k effectively acts as a secret key that governs both spatial and spectral embedding patterns.

During the extraction phase, the same Rademacher function is applied to the stego-image, ensuring that the channel selection and pixel positions are reproduced exactly. This guarantees full reversibility of the embedding process and enables reliable recovery of the hidden message.

5.1 Rademacher pixel selection for color images

The Figure 3 illustrates the application of discrete Rademacher vectors to a small color image. In this example, pixel positions corresponding to $+1$ entries are marked in green, while -1 entries are marked in blue.

The orthogonal and pseudo-random-like distribution of pixel positions ensures deterministic embedding while minimizing visible artifacts in the host image.

By exploiting both spatial position and color-channel structure, this method can be naturally extended to larger images and multiple Rademacher vectors for embedding longer messages. Importantly, the same Rademacher-based selection principle can be visualized in alternative but mathematically equivalent forms.

Figure 4 presents an alternative color-coded layout derived from a different grouping and ordering of Rademacher-like patterns across image rows. These alternative visual representations do not alter the underlying mathematical properties of the Rademacher functions.

Instead, they provide additional flexibility in practical implementations, allowing the designer to adapt the embedding pattern to perceptual constraints, robustness requirements, or implementation simplicity. Such flexibility is particularly advantageous in color image steganography, where visual transparency and controlled distribution of modified pixels are critical.

5.2 Function selection and embedding agreement

It should be noted that the proposed method does not use Rademacher functions as cryptographic keys in the classical sense. Instead, the sender and receiver agree in advance on the particular Rademacher or Walsh function used to determine pixel positions and, in the case of color images, the selection of embedding channels. Therefore, the method should be viewed as a deterministic embedding strategy rather than an encryption mechanism.

For the considered images of size 512×512, the practical choice of a single Rademacher function is naturally limited by the image dimensions. In the present work, the function R_8 was employed, since it generates

$$2^{8+1} = 512$$

alternating intervals, which corresponds to the image dimension. Although higher-order Rademacher functions can be defined mathematically, for example R_9, which partitions the interval $[0, 1)$ into 1024 alternating subintervals, such functions were not considered in the present implementation.

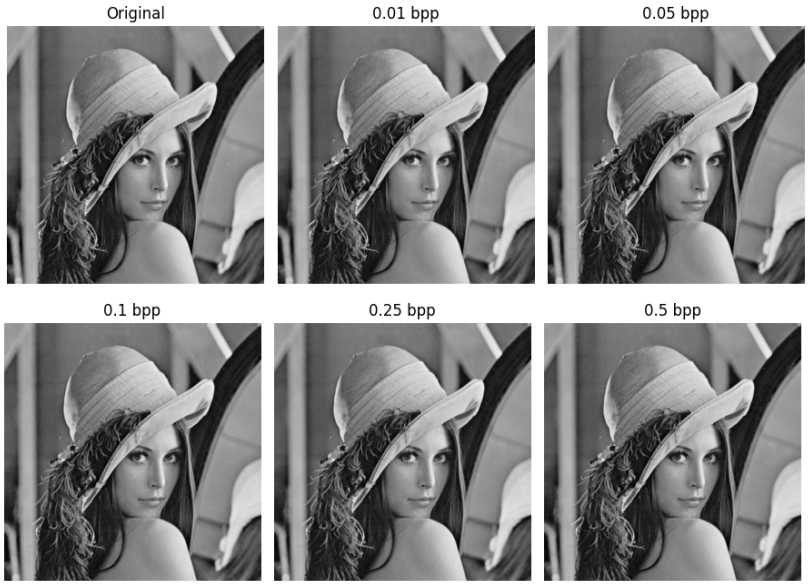

Figure 5: Grayscale stego-images of the Lena dataset under different embedding rates.

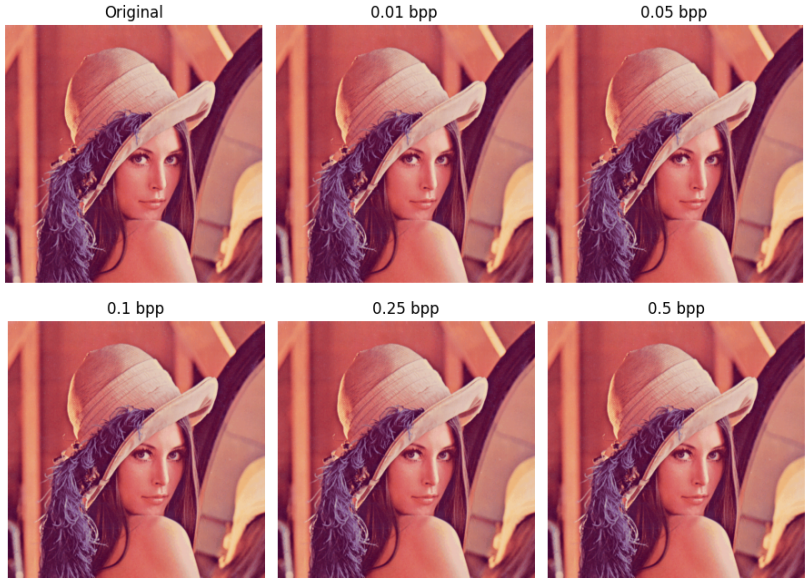

Figure 6: Color stego-images of the Lena dataset under different embedding rates.

At the same time, the embedding pattern is not restricted to a single Rademacher function. As discussed in Section 3.1, Walsh functions can be constructed as finite products of Rademacher functions. For example,

$$W_{81}(x) = R_6(x)R_4(x)R_0(x),$$

since

$$81 = 2^6 + 2^4 + 2^0.$$

Consequently, different Walsh functions may be selected to generate alternative embedding patterns. More generally, combinations such as

$$W_u(x)W_v(x)W_w(x)W_y(x)$$

can also be employed to determine pixel locations and color-channel selection. Therefore, the exact embedding pattern depends on the prior agreement between the communicating parties regarding the function or function combination used during embedding and extraction. This flexibility provides multiple deterministic embedding configurations while preserving the reproducibility of the extraction process.

6 Experimental results and steganographic quality assessment

The well-known Lena image of size 512×512 is used as a benchmark for evaluating the proposed Rademacher-based steganographic scheme. Both grayscale and color versions of the image are considered in order to analyze the effect of embedding across different signal representations.

The embedding process modifies the least significant bits (LSBs) of selected pixels according to the Rademacher function $R_8(n)$, while maintaining high perceptual fidelity of the host image. Four experimental scenarios are evaluated using different payload rates:

$$\text{BPP} \in \{0.01,\ 0.05,\ 0.1,\ 0.25,\ 0.5\}.$$

Figure 5 presents the grayscale stego-images obtained at different payload capacities. As observed, even at higher embedding rates, the structural integrity of the image is preserved with minimal visible distortion.

Figure 6 shows the corresponding results for the color Lena image. The embedding is performed in the Blue and Green channels according to the sign of the Rademacher function, while the Red channel remains unchanged to minimize perceptual distortion.

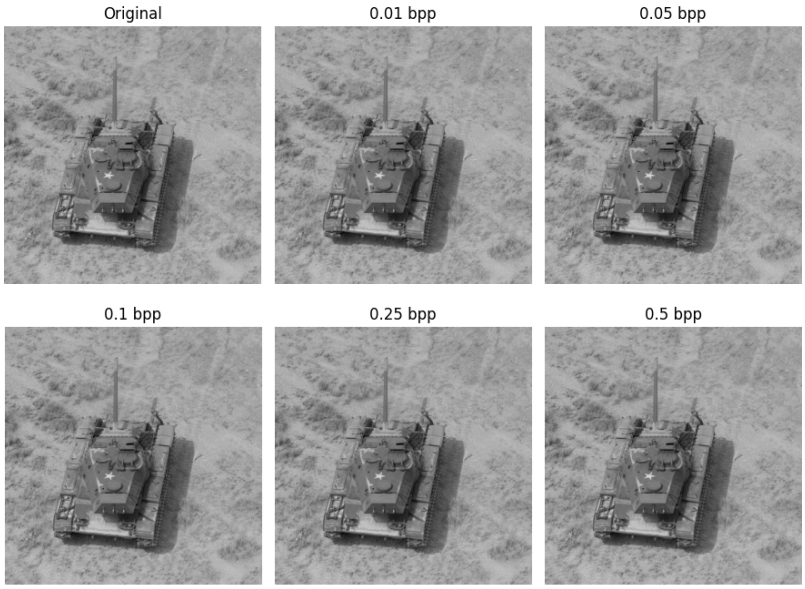

Figure 7: Grayscale stego-images of the Tank dataset under different embedding rates.

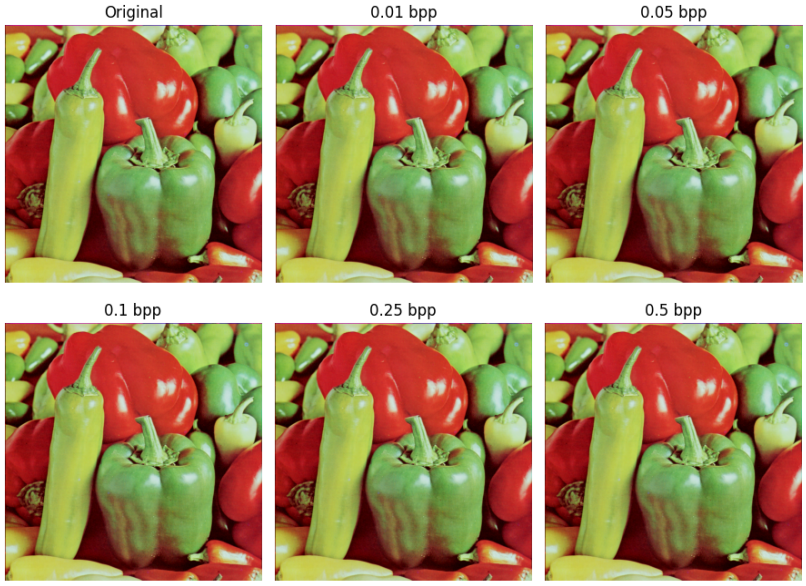

Figure 8: Color stego-images of the Pepper dataset under different embedding rates.

6.1 Peak Signal-to-Noise Ratio (PSNR)

The Peak Signal-to-Noise Ratio (PSNR) is defined as:

$$\text{PSNR} = 10 \log_{10} \left(\frac{255^2}{\text{MSE}} \right),$$

where the Mean Squared Error (MSE) is:

$$\text{MSE} = \frac{1}{HW} \sum_{i=1}^{H} \sum_{j=1}^{W} \Big(I(i,j) - \hat{I}(i,j) \Big)^2 .$$

In the case of color images, the error is computed jointly over all three RGB channels. Let the original image be denoted as $I^c(i,j)$ and the stego image as $\hat{I}^c(i,j)$, where $c \in \{R, G, B\}$. Then the Mean Squared Error for color images is defined as:

$$\text{MSE} = \frac{1}{3HW} \sum_{c \in \{R,G,B\}} \sum_{i=1}^{H} \sum_{j=1}^{W} \Big(I^c(i,j) - \hat{I}^c(i,j) \Big)^2 .$$

Accordingly, the PSNR for color images is given by:

$$\text{PSNR} = 10 \log_{10} \left(\frac{255^2}{\text{MSE}} \right).$$

6.2 Structural Similarity Index (SSIM)

The Structural Similarity Index (SSIM) [7–9] is a perceptual metric used to measure the similarity between the original image and the stego image. Unlike pixel-wise error measures, SSIM evaluates structural information, luminance, and contrast simultaneously.

For grayscale images, SSIM is defined as:

$$\text{SSIM}(x,y) = \frac{(2\mu_x\mu_y + C_1)(2\sigma_{xy} + C_2)}{(\mu_x^2 + \mu_y^2 + C_1)(\sigma_x^2 + \sigma_y^2 + C_2)},$$

where μ_x and μ_y are the mean intensities of the original and stego images, σ_x^2 and σ_y^2 are their variances, and σ_{xy} is the covariance between them. The constants C_1 and C_2 are small values used to stabilize the division.

For color images, SSIM is computed by extending the same formulation to the three RGB channels. Let x^c and y^c denote the corresponding color channels, where $c \in \{R, G, B\}$. Then SSIM is evaluated per channel as:

$$\text{SSIM}_c = \frac{(2\mu_x^c \mu_y^c + C_1)(2\sigma_{x^c y^c} + C_2)}{((\mu_x^c)^2 + (\mu_y^c)^2 + C_1)((\sigma_{x^c}^2 + \sigma_{y^c}^2 + C_2)},$$

and the final SSIM value for the color image is obtained by averaging over all channels:

$$\text{SSIM} = \frac{1}{3} \sum_{c \in \{R,G,B\}} \text{SSIM}_c.$$

6.3 Discussion of experimental results

The experimental results Table 1 demonstrate a consistent trade-off between embedding capacity and visual quality. As the payload increases, the PSNR values decrease for both grayscale and color images, which is expected due to higher distortion introduced by embedding a larger number of bits into the Least Significant Bits (LSBs). However, the Structural Similarity Index (SSIM) remains extremely high across all payload levels, staying close to 1. This indicates that although pixel-level differences increase, the overall structural information of the image is preserved.

In comparison, color images consistently achieve higher PSNR values than grayscale images. This improvement is attributed to the distribution of embedded data across multiple color channels, which reduces the perceptual impact on any single channel. In particular, the Rademacher-controlled selection of Green and Blue channels further balances distortion across the image. Overall, the results confirm that the proposed Rademacher-based steganographic method maintains high imperceptibility and structural fidelity even at relatively high embedding capacities, making it suitable for secure image data hiding applications.

6.4 Computational complexity analysis of the proposed Rademacher-based LSB method

The proposed Rademacher-based Least Significant Bit (LSB) steganographic method exhibits linear computational complexity with respect to the number of pixels in the host image. Let N denote the total number of pixels and L the number of embedded payload bits. In the classical sequential LSB approach, the embedding procedure traverses the image in a linear scan and modifies the

Payload (bpp)	Image Type	PSNR (dB)	SSIM
0.01	Grayscale	71.16	0.999959
0.01	Color	75.90	0.999995
0.05	Grayscale	64.07	0.999731
0.05	Color	68.97	0.999961
0.10	Grayscale	61.14	0.999513
0.10	Color	65.95	0.999919
0.25	Grayscale	57.19	0.998908
0.25	Color	61.94	0.999816
0.50	Grayscale	54.16	0.997840
0.50	Color	58.95	0.999679

Table 1: Performance evaluation of Rademacher-based steganography for grayscale and color images.

least significant bit of each pixel until all L message bits are embedded. Consequently, the computational cost is proportional to the payload size, yielding a time complexity of $O(L)$. In the worst-case scenario, when the payload occupies the maximum embedding capacity of the image ($L \approx N$), the complexity reduces to $O(N)$.

In contrast, the proposed method introduces a deterministic selection mechanism based on the Rademacher function $R(n)$, which partitions the pixel index space into two alternating subsets. The embedding process requires a complete traversal of all N pixels in order to evaluate the Rademacher condition and determine whether a given pixel is eligible for embedding. Each evaluation of $R(n)$ is computationally constant, and the subsequent least significant bit modification is also performed in constant time. Therefore, the total computational complexity of the proposed algorithm is $O(N)$, independent of the actual payload size, as the full image scan is always required.

7 Comparative analysis of Rademacher-based and sequential LSB steganography

In this chapter, we evaluate the performance of the proposed Rademacher-based steganographic method in comparison with the classical sequential Least Significant Bit (LSB) approach. The experiments are conducted on two benchmark images: the grayscale *Tank* image and the color *Pepper* image, both of resolution 512×512 pixels.

Payload (bpp)	Image Type	PSNR (dB)	SSIM
0.01	Grayscale (Tank)	71.11	0.999978
0.01	Color (Pepper)	75.85	0.999997
0.05	Grayscale (Tank)	64.16	0.999851
0.05	Color (Pepper)	68.91	0.999963
0.10	Grayscale (Tank)	61.11	0.999691
0.10	Color (Pepper)	65.91	0.999907
0.25	Grayscale (Tank)	57.15	0.999219
0.25	Color (Pepper)	61.95	0.999695

Table 2: Performance of Rademacher-based LSB steganography on Tank and Pepper images.

Payload (bpp)	Image Type	PSNR (dB)	SSIM
0.01	Grayscale (Tank)	70.94	0.999986
0.01	Color (Pepper)	71.15	0.999976
0.05	Grayscale (Tank)	64.17	0.999866
0.05	Color (Pepper)	64.16	0.999832
0.10	Grayscale (Tank)	61.12	0.999709
0.10	Color (Pepper)	61.15	0.999662
0.25	Grayscale (Tank)	57.16	0.999279
0.25	Color (Pepper)	57.17	0.999174

Table 3: Performance of Sequential LSB steganography on Tank and Pepper images.

The grayscale case corresponds to the *Tank* image, while the color case corresponds to the *Pepper* image. Identical payload levels (0.01, 0.05, 0.1, 0.25, and 0.5 bits per pixel) were used for both methods to ensure a fair comparison.

Figures 7 and 8 illustrate the stego-images obtained using the proposed Rademacher-based method for grayscale and color images, respectively.

7.1 Experimental results

The numerical results for both methods are summarized in Tables 2 and 3. For each payload level, we report the number of embedded bits, Peak Signal-to-Noise Ratio (PSNR), and Structural Similarity Index (SSIM).

8 Conclusion

In this work, a novel steganographic approach based on discrete Rademacher functions was proposed and investigated for both grayscale and color images. Unlike conventional sequential Least Significant Bit (LSB) embedding, the proposed method employs Rademacher functions to control the selection of embedding locations and, in the case of color images, the choice of embedding channels. This introduces a deterministic yet non-sequential embedding pattern that increases the complexity of unauthorized message detection. A detailed mathematical formulation of the embedding and extraction procedures was presented.

The proposed approach was evaluated using standard benchmark images, including Lena, Tank, and Pepper images with a resolution of 512×512 pixels. The quality of the resulting stego-images was assessed using two widely accepted image quality metrics: Peak Signal-to-Noise Ratio (PSNR) and Structural Similarity Index (SSIM).

The experimental results demonstrated that the proposed method preserves excellent visual quality over a wide range of embedding rates. Even at relatively high payloads, the obtained PSNR values remained well above commonly accepted steganographic quality thresholds, while SSIM values stayed extremely close to unity, indicating negligible perceptual degradation and strong preservation of image structure.

Comparative experiments with the classical sequential LSB method revealed that the proposed Rademacher-based approach achieves comparable or slightly improved visual quality, particularly for color images where the embedding process is distributed between the Green and Blue channels according to the sign of the Rademacher function. From a computational perspective, the proposed algorithm exhibits linear time complexity, $O(N)$, with respect to the number of image pixels, making it computationally efficient and suitable for practical applications.

The deterministic nature of the Rademacher-based selection mechanism also ensures reliable and lossless message extraction when the stego-image remains unaltered. Overall, the obtained results confirm that Rademacher-controlled LSB steganography provides an effective balance between embedding capacity, visual imperceptibility and computational efficiency. These characteristics make the proposed method a promising alternative to traditional LSB techniques for secure image information hiding.

Future research may focus on extending the proposed framework to adaptive Rademacher-based embedding strategies, multi-level bit-plane embedding, transform-domain steganography, and robustness evaluation under image processing operations such as compression, filtering, scaling, and noise contamination.

References

[1] N. Provos, P. Honeyman, Hide and seek: an introduction to steganography, *IEEE Security & Privacy*, 1:32–44, 2003.

[2] F. A. P. Petitcolas, S. Katzenbeisser, *Information hiding techniques for steganography and digital watermarking*, Artech House Computer Security Series, Artech House, 2000.

[3] R. Chandramouli, N. Memon, Analysis of LSB based image steganography techniques, *Proceedings 2001 International Conference on Image Processing*, 3:1019–1022, IEEE, 2001.

[4] J. Mielikainen, LSB matching revisited, *IEEE Signal Processing Letters*, 13:285–287, 2006.

[5] F. J. MacWilliams, N. J. A. Sloane, *The Theory of Error-correcting Codes*, Elsevier, 1977.

[6] A. V. Oppenheim, *Discrete-time signal processing*, Pearson Education India, 1999.

[7] Z. Wang, A. C. Bovik, H. R. Sheikh, E. P. Simoncelli, Image quality assessment: from error visibility to structural similarity, *IEEE Transactions on Image Processing*, 13:600–612, 2004.

[8] Z. Wang, A. C. Bovik, Mean squared error: Love it or leave it? A new look at Signal Fidelity Measures, *IEEE Signal Processing Magazine*, 26:98–117, 2009.

[9] A. Horé, D. Ziou, Image Quality Metrics: PSNR vs. SSIM, *2010 20th International Conference on Pattern Recognition*, pp. 2366–2369, IEEE, 2010.